Accelerated Publications

An Oscillating Manganese Electron Paramagnetic Resonance Signal from the S_0 State of the Oxygen Evolving Complex in Photosystem II†

Karin A. Åhrling, Sindra Peterson, and Stenbjörn Styring*

Department of Biochemistry, Center for Chemistry and Chemical Engineering, Lund University, P.O. BOX 124, S-221 00 Lund, Sweden

Received July 28, 1997; Revised Manuscript Received September 11, 1997⊗

ABSTRACT: Photosynthesis produces the oxygen necessary for all aerobic life. During this process, the manganese-containing oxygen evolving complex (OEC) in photosystem II (PSII), cycles through five oxidation states, S_0-S_4. One of these, S_2, is known to be paramagnetic and gives rise to electron paramagnetic resonance (EPR) signals used to probe the catalytic structure and function of the OEC. The S_0 state has long been thought to be paramagnetic. We report here a Mn EPR signal from the previously EPR invisible S_0 state. The new signal oscillates with a period of four, indicating that it originates from fully active PSII centers. Although similar to the S_2 state multiline signal, the new signal is wider (2200 gauss compared with 1850 gauss in samples produced by flashing), with different peak intensity and separation (82 gauss compared with 89 gauss). These characteristics are consistent with the S_0 state EPR signal arising from a coupled $Mn^{II}-Mn^{III}$ intermediate. The new signal is more stable than the S_2 state signal and its decay in tens of minutes is indicative of it originating from the S_0 state. The S_0 state signal will provide invaluable information toward the understanding of oxygen evolution in plants.

Photosystem II (PSII)[1] in plants, green algae, and cyanobacteria catalyzes the light-driven oxidation of water to molecular oxygen. The active site, the oxygen evolving complex (OEC), contains four Mn atoms (*1*−*3*). The OEC cycles through five redox intermediates, the S states, S_0-S_4 (*4*), labeled according to the number of positive redox equivalents stored. These states mostly reflect oxidation of Mn atoms. However, ligand oxidation is thought to occur on the S_2-S_3 step (*3*, *5*). The S_4 state is very short-lived and corresponds to the release of dioxygen from the catalytic site. The S_2 state is paramagnetic and gives rise to the electron paramagnetic resonance (EPR) multiline signal (*6*), a complex hyperfine structured signal, as well as a broad signal centered around $g = 4.1$ (*1*, *2*). The S_2 state also shows several other EPR spectra in inhibited or perturbed PSII centers. Other states are also EPR active. The S_1 state gives rise to a parallel polarized EPR signal (*7*), while the S_3 state shows a split radical signal in partially inhibited systems (*8*), which has been ascribed to a radical interacting with the Mn cluster. These EPR signals are informative and their detailed spectroscopic characterization has provided valuable insight into the structure and function of the Mn cluster. Of all these EPR signals from the OEC, only the S_2 state multiline and $g = 4.1$ signals represent fully active samples that oscillate through the S cycle.

There has not yet been any report of an EPR signal from the S_0 state, which for long has been predicted to be paramagnetic (*5*). To reach the S_0 state, three flashes of light are required. For each flash, misses and double hits scramble the S states such that the amount of signal in an S_0 sample may be low (especially in concentrated EPR samples). For this reason, the S_0 state is the most difficult to study experimentally.

In this study we have combined a preflash protocol with powerful laser flashes to synchronize the samples, which ensures a high concentration of the S_0 state after three flashes. This allows us to report here the first observation of an oscillating EPR signal from the S_0 state of PSII. The signal is observed in oxygen evolving PSII samples, it oscillates as the S_0 state of the Mn cluster, and it is very stable compared to the multiline EPR signal in the S_2 state.

EXPERIMENTAL PROCEDURES

PSII-enriched membrane fragments were prepared from spinach as in Pace *et al.* (*9*). Oxygen evolution was measured using a Clark oxygen electrode with phenyl-p-benzoquinone (PPBQ) as electron acceptor.

EPR samples were made up to 3.5 mg of Chl mL^{-1} in a buffer containing 400 mM sucrose, 15 mM NaCl, 10 mM $MgCl_2$, 20 mM MES, pH 6.0, with or without 3% methanol. The samples, in calibrated EPR tubes, were incubated in the dark for 10 min at room temperature and given a saturating flash from a Nd:YAG laser (6 ns, 300 mJ, 532 nm). After the preflash, given in the absence of electron acceptors to allow efficient recombination, the samples were left to equilibrate at room temperature in the dark for 15 min. This preflash treatment synchronizes the PSII centers in the S_1

† This work was supported by the Swedish National Science Research Council, the Knut and Alice Wallenberg Foundation, and the Crafoord Foundation.

⊗ Abstract published in *Advance ACS Abstracts,* October 15, 1997.

[1] Abbreviations: Chl, chlorophyll; DMSO, dimethyl sulfoxide; EPR, electron paramagnetic resonance; OEC, oxygen evolving complex; PPBQ, phenyl-p-benzoquinone; PSII, photosystem II; Y_D, tyrosine D.

S0006-2960(97)01815-1 CCC: $14.00

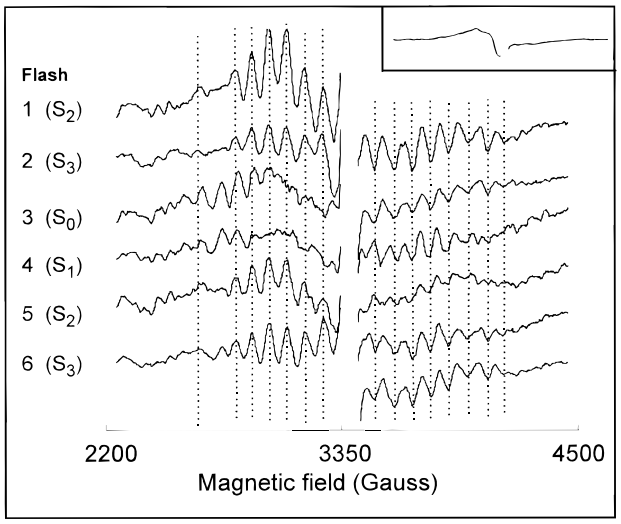

FIGURE 1: Flash dependence of EPR signals in PSII membranes, illuminated minus dark spectra. The number of flashes and the dominating S states after flashes are indicated. Vertical guidelines indicate S_2 peak positions. The EPR signal from the dark stable Y_D radical (*12*) in the central region of the spectra has been removed. Inset shows the dark spectrum after preflash treatment and PPBQ addition. EPR settings: frequency, 9.47 GHz; power, 5.9 mW; modulation amplitude, 20 G; modulation frequency, 100 kHz; temperature, 7 K.

state (*10*). It also results in complete oxidation of Y_D (signal II slow) (*11*). One minute before the next set of flashes, 0.5 mM PPBQ in dimethyl sulfoxide (DMSO) was added to the samples as electron acceptor. The flashed samples were frozen within 1 s in an ethanol/solid CO_2 bath and transferred to liquid nitrogen (*10*). For the study of the decay of the S_2 multiline and the S_0 signal the samples remained in the dark at room temperature for the indicated time prior to freezing.

Continuous wave EPR spectra were recorded at liquid helium temperatures with a Bruker 380E spectrometer fitted with an Oxford Instruments cryostat. Spectrometer conditions are given in the figure captions.

RESULTS AND DISCUSSION

Our studies were performed in samples containing methanol, which have been observed to yield, in the S_2 state, the unmodified multiline EPR signal exclusively (*9*).

Figure 1 shows the flash dependent EPR spectra recorded in these PSII samples. It is clear that the S_2 multiline EPR signal is large on the first flash. Then, as expected, it decreases in size, to again increase in size on the fifth flash, but this oscillation does not appear very deep; all samples have significant multiline signals. However, a thorough inspection of the spectra reveals a different picture: the overall spectral shape is different in the third and fourth flash samples compared with the other samples. The peaks of the conventional first flash (S_2) multiline signal have been indicated by lines throughout the spectra. These lines match the peaks of the spectrum after two flashes where a fraction of S_2 remains, see Figure 2. After three flashes, where the S_0 state should dominate, there is a significant change in the position of the peaks. The shift remains in the fourth flash spectrum. The fifth flash spectrum is again dominated by the S_2 state, and here the S_2 state peak pattern returns. This pattern is sustained in the sixth flash spectrum.

The result is quite unexpected. In a similar study of samples without the addition of methanol, we obtained the

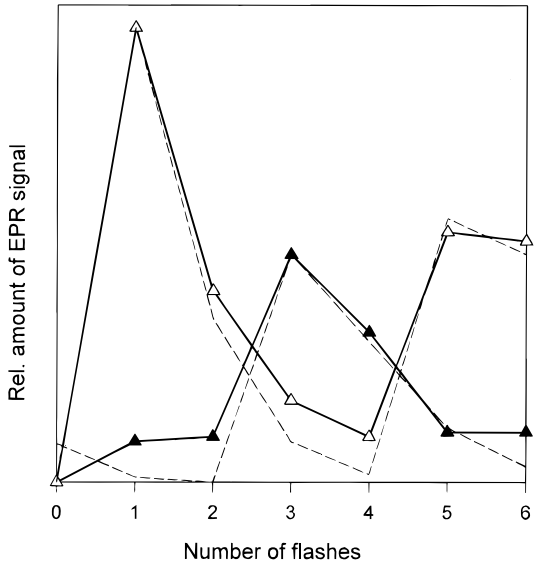

FIGURE 2: Relative yield of the S_0 (▲) and S_2 (Δ) signals vs flash number, as measured on peaks indicated in Figure 4. The dashed curves give the simulated S_0 and S_2 populations assuming 10% S_0 in preflashed samples and 13% misses on each flash.

S_2 multiline EPR signal only, which oscillated deeply with the flash number. The amplitude was very large on the first and the fifth flashes and almost zero on the third and fourth flashes (not shown). The observed oscillations could be fitted assuming that all centers were in the S_1 state initially (after the preflash), and that the flashes induced 10% misses and no double hits. This study confirmed that the laser flash was saturating the sample and hence that the very different oscillation behavior seen in the methanol-containing samples was not produced by an artefact of the flash. Furthermore, the addition of methanol did not alter the oxygen evolving capacity of the samples, which was 400 μM O_2/mg of Chl/h with or without 3% methanol.

In the third flash (S_0) and fourth flash samples presented here (Figure 1), the region below 3300 gauss shows intensity where the first flash (S_2 multiline signal) does not. Upfield of this region, the peaks appear closer together than in the S_2 multiline. Note also the relatively intense peaks at the edges of the third flash spectrum. Already this analysis indicates the presence of a novel EPR signal in the third and fourth flash spectra.

At first sight, however, the EPR signals of the S_2 and S_0 states appear similar. It was therefore necessary to distinguish them from each other. The stability of the S_2 and S_0 states are known to be different, the S_0 state being about 10 times more stable than the S_2 state (*13*). We used this property to assign the new EPR signal. The decay at room temperature of the two signals, after one and three flashes, respectively, is shown in Figure 3. The study clearly shows that the signals can be attributed to two different states of the OEC. The S_2 state multiline signal in these samples decays with a half-time of 1.5 min. In contrast, the decay of the S_0 state signal shows a half-time of 12 min. The initial behavior of the S_0 decay is due to relaxation of centers in S_2 and S_3.

We also investigated whether the signal returned on the second turnover by studying the highly scrambled seventh and eighth flash samples (Figure 4, eighth flash). In both cases we identified a multitude of peaks belonging to the S_0 state signal. However, these signals have significant con-

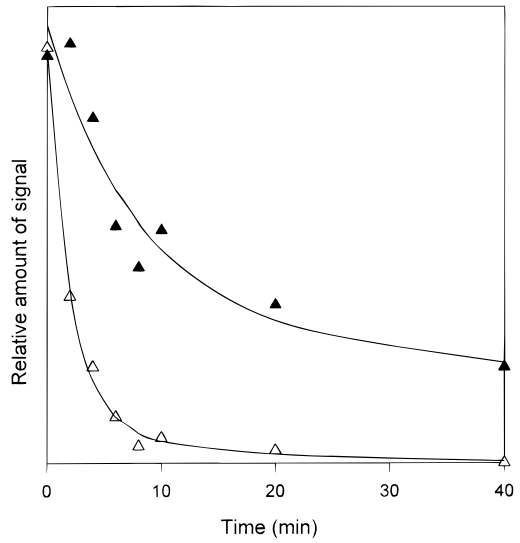

FIGURE 3: Decay of S_0 (▲) and S_2 (Δ) state EPR signal intensities with time, recorded in samples given three and one flashes, respectively. The flashed samples were incubated in the dark at room temperature for the indicated periods of time prior to freezing. The curves represent exponential fits with decay half-times of 12 and 1.5 min, respectively.

tributions of S_2 multiline signal (about 20% in the seventh flash sample) which, on a spin basis, is dominated by considerably more intense hyperfine lines than those of the S_0 state signal. Nevertheless, by subtracting out the S_2 multiline signal from the eighth flash spectrum, which has a smaller proportion of centers in the S_2 state, the S_0 spectrum became very apparent (Figure 4). The novel EPR signal evidently oscillates with the S_0 state as it returns with the second turnover of the enzyme. Furthermore, the signal can clearly be assigned to the S_0 state since it could be developed by the addition of methanol after the flash treatment, where, in the absence of methanol, no S_0 signal was observed.

The above identification was further corroborated by our attempts to analyze the oscillation pattern of the EPR signals in the methanol-treated samples (Figure 2). By calculating the oscillation pattern using three strong peaks (Figure 4, Δ) from the first flash spectrum, we obtained deep oscillations (Figure 2, Δ) corresponding to the cycling of the S_2 state population. This oscillation is similar to that obtained in standard sucrose samples. If we instead use three strong peaks (Figure 4, ▲) from the third flash spectrum, the oscillation obtained is completely different (Figure 2, ▲), following the expected S_0 population. The dashed lines of Figure 2 are the S_0 and S_2 population oscillations, calculated with a 13% miss factor and 10% S_0 in the preflashed state. In measuring S_0 peak amplitudes, no correction for underlying S_2 amplitude was made (Figure 4). This is reflected in small experimental deviations from the simulations (Figure 2).

From these observations we conclude that the S_0 state gives rise to an EPR signal similar to, but distinct from, the S_2 state multiline signal. This new EPR signal originates from a fully active oxygen evolving PSII complex. It also oscillates with a period of four which is indicative of it originating from the OEC.

Figure 4 shows the S_0 state EPR signal produced by three flashes, together with the S_2 state multiline spectrum produced by one flash and the S_0 state signal produced by eight flashes, discussed above. The observable S_2 multiline signal is about 1850 gauss in the flashed samples. The S_0 signal appears to be at least 20% wider. The figure highlights the peaks in the wings of the spectrum that we so far have reproduced with certainty. The S_0 state signal exhibits several additional peaks with an average peak separation for the major peaks of 82 gauss compared with 89 gauss in the S_2 state signal.

In the region below 3300 gauss, the peak separation is a little less than in the S_2 multiline signal and the relative intensities of the peaks in the two spectra are quite different; in the S_0 spectrum the more intense peaks lie further to the edge of the spectrum. It is worth noting that the relative intensity of the smaller peaks at the edges of the spectrum vary both in the upfield and downfield portion of the spectra.

Above 3500 gauss the peak separation of the S_0 signal is considerably less than that of the S_2 signal, with an average spacing of 83 gauss between the major peaks, compared with 92 gauss. Additional peaks at the edge of the spectrum are also apparent (inset, Figure 4). The edge peaks which we can reproduce with confidence have been marked in the spectrum.

The S_0 state signal presented here has a clear contribution from an underlying broad component, whereas the S_2 state signal appears to have very little. The origin of this broad signal is under investigation. It should be noted that the S_2 state spectrum under these conditions has no contribution from the excited state $g = 4.1$ signal (see inset in Figure 4) as is expected (*9*). The S_0 state spectrum also showed no contribution in the $g = 4$ region in the temperature range 5−25 K.

The mechanism whereby methanol affects the Mn cluster in the OEC is not known and potentially of large mechanistic and structural interest. However, it seems clear that methanol interacts closely with the cluster. It was recently observed that methanol eliminates the S_1 state parallel polarized EPR signal (*14*). In addition, the EPR signals from the Mn cluster are much modified in S_2 (*9*) and S_0 (this study). This may reflect ligand substitution or conformational changes in the vicinity of the Mn. Studies of synthetic Mn complexes might elucidate the phenomenon. For instance, an ESEEM study indicates that methanol replaces water bound to a Mn^{III}−Mn^{IV} dimer (*15*).

Alternative multiline signals from the S_2 state in perturbed systems have, as a rule, more lines and smaller line spacing than the normal S_2 state multiline signal. The multiline signal arising from a preparation depleted of Ca^{2+} shows a peak separation of 55 gauss (*8*). Sr^{2+} replacement (*16*) gives rise to a signal with average line spacing of about 71 gauss. Similarly the NH_4Cl-treated PSII membranes (*17*) have an EPR signal with average spacing of 67.5 gauss. However, none of these signals is wider than the normal S_2 state multiline signal. Thus, it is unlikely, from this analysis, that the signal (Figure 4) observed in the third flash sample (S_0) results from a perturbed state; this is corroborated by the high activity and good oscillation pattern of the EPR signals in our samples (Figure 2).

The S_2 state multiline signal is thought to stem from a $Mn^{III}(Mn^{IV})_3$ oxidation state of the OEC, where the redox active center is a di-μ-oxo bridged Mn^{III}−Mn^{IV} (*3*). The characteristic EPR multiline pattern would arise from an antiferromagnetically coupled redox active dimer, yielding a state with one net unpaired electron, $S = {}^1/_2$ (*18*, *19*). The participation of the other two Mn ions in the formation of

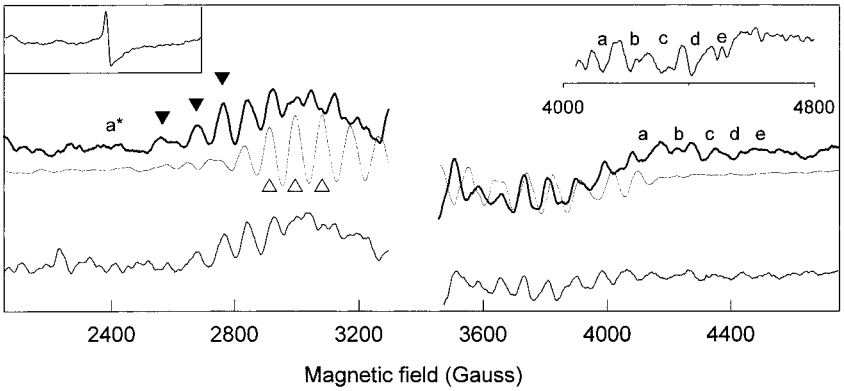

FIGURE 4: S_0 state EPR signal (bold line) produced by three flashes, together with the S_2 state multiline signal (fine line) produced by one flash, and the 8 flash S_0 state signal (normal line), illuminated minus dark spectra. The three flash S_0 state spectrum has had the 8% contribution of S_2 state multiline (Figure 2) subtracted from it. The S_2 spectrum has been scaled to $^1/_4$ of its actual size. The radical region has been omitted. Inset left: $g = 4.1$ region from the S_2 state. ▲ and Δ indicate peaks used in calculation of oscillation patterns for S_0 and S_2, respectively (Figure 2). Inset right: high-resolution spectrum of S_0 edge. Letters indicate reproducible S_0 edge peaks. In the eighth flash sample, the S state population is highly scrambled. We have therefore, in the presented spectrum, subtracted a substantial amount (≈15%) of the S_2 multiline signal to highlight the population of S_0 in the sample. The spectral intensity is on a different scale to the three-flash S_0 state signal. EPR settings: frequency, 9.47 GHz; power, 14 mW (inset right 28 mW); modulation amplitude, 20 G, modulation frequency, 100 kHz, temperature, 7 K.

the S_2 state signal is debated. However there seems to be general agreement that these two Mn ions are redox inactive (*3*, *5*). The S_0 state represents a state with two more electrons. As Mn-oxidation is thought to occur on the steps from S_0 to S_2 (*1*, *2*), the most likely oxidation state for the redox active dimer is $Mn^{II}-Mn^{III}$ (*3*). Such a system may be modeled by assuming an effective spin Hamiltonian where the intrinsic hyperfine interactions are scaled by projection operators (*18*, *19*). The projection operators for a $Mn^{III}-Mn^{IV}$ dimer are $2a_{III}$ and $-1a_{IV,}$ where a stands for the intrinsic hyperfine interaction for the ion in question. The projection operators for a $Mn^{II}-Mn^{III}$ dimer are $^7/_3a_{II}$ and $-^4/_3a_{III}$ (*20*). Assuming the same magnitude of the intrinsic hyperfine interaction for each Mn atom, regardless of oxidation state, the width of the spectrum, based on projection operators for the two systems, indicates that a $Mn^{II}-Mn^{III}$ dimer will be 22% larger than that of the $Mn^{III}-Mn^{IV}$. For the Mn cluster in PSII this would correspond to a width of 2200 gauss. The intrinsic hyperfine interaction for Mn^{II} is often larger than for Mn^{III} and Mn^{IV} (*21*, *22*). A study of the Mn-catalase enzyme (*23*) shows that the $Mn^{II}-Mn^{III}$ form has an EPR signal which is 42% wider than the $Mn^{III}-Mn^{IV}$ form. Simulations show that the additional 20% of the width can be accounted for by increased hyperfine magnitude in Mn^{II}. The width of 2400 gauss is approximately consistent with the S_0 spectrum presented here, which is at least 2200 gauss wide in flashed samples. It should be noted that in our experience the observable spectral width of the S_2 multiline signal is several 100 gauss smaller in a flashed sample, where the signal-to-noise ratio is smaller due to the lower sample concentration compared with a continuously illuminated, high concentration sample (*19*). It is likely that the same holds for the S_0 signal and a detailed analysis to determine the actual width of the spectrum in more dense samples is in progress. A knowledge of the actual width of the spectrum will allow a determination of the relative intensities of the S_0 and S_2 state signals.

Concluding, we have found that the S_0 state of the Mn cluster is paramagnetic and gives rise to an EPR signal which oscillates with a period of four. Although similar to the S_2 multiline, the new signal is wider, with different peak intensity and separation, and more long-lived. Supporting earlier results (*5*, *24*, *25*), the spectral properties are strongly indicative of a Mn cluster with the redox-active part in a $Mn^{II}-Mn^{III}$ oxidation state.

NOTE ADDED IN PROOF

After submission of this manuscript we became aware of a report of an S_0* state EPR signal produced by reduction of the S_1 state (*26*). This signal is very similar to the S_0 signal presented here, which oscillates with flash number. The S_0 signal has now also been produced in PSII samples that were given three flashes (J. Messinger, personal communication).

ACKNOWLEDGMENT

The authors acknowledge valuable discussions with Y. Frapart, A. Magnuson, F. Mamedov. We thank J. Messinger for copies of his manuscripts prior to publication.

REFERENCES

1. Rutherford, A. W. (1989) *Trends Biol. Sci. 14*, 227−232.
2. Debus, R. J. (1992) *Biochim. Biophys. Acta 1102*, 269−352.
3. Yachandra, V. K., Sauer, K., and Klein, M. P. (1996) *Chem. Rev. 96*, 2927−2950.
4. Kok, B., Forbush, B., and McGloin, M. (1970) *Photochem. Photobiol. 11*, 457−475.
5. Styring, S., and Rutherford, A. W. (1988) *Biochemistry 27*, 4915−4923.
6. Dismukes, G. C., and Siderer, Y. (1981) *Proc. Natl. Acad. Sci. U.S.A. 78*, 274−278.
7. Dexheimer, S. L., and Klein, M. P. (1992) *J. Am. Chem. Soc. 114*, 2821−2826.
8. Boussac, A., Zimmermann, J.-L., and Rutherford, A. W. (1989) *Biochemistry 28*, 8984−8989.
9. Pace, R. J., Smith, P., Bramley, R., and Stehlik, D. (1991) *Biochim. Biophys. Acta 1058*, 161−170.
10. Styring, S., and Rutherford, A. W. (1987) *Biochemistry 26*, 2401−2405.
11. Styring, S., and Rutherford, A. W. (1988) *Biochim. Biophys. Acta 933*, 378−387.
12. Barry, A. B., and Babcock, G. T. (1987) *Proc. Natl. Acad. Sci. U.S.A. 84*, 7099−7103.
13. Vass, I., and Styring, S. (1991) *Biochemistry 30*, 830−839.
14. Yamauchi, T., Mino, H., Matsukawa, T., Kawamori, A., and Ono, T. (1997) *Biochemistry 36*, 7520−7526.

15. Randall, D. W., Gelasco, A., Caudle, M. T., Pecoraro, V. L., and Britt, R. D. (1997) *J. Am. Chem. Soc. 119*, 4481−4491.
16. Boussac, A., and Rutherford, A. W. (1988) *Biochemistry 27*, 3476−3483.
17. Beck, W. F., de Paula, J. C., and Brudvig, G. W. (1986) *J. Am. Chem. Soc. 108*, 4018−4022.
18. Randall, D. W., Sturgeon, B. E., Ball, J. A., Lorigan, G. A., Chan, M. K., Klein, M. P., Armstrong, W. H., and Britt, R. D. (1995) *J. Am. Chem. Soc. 117*, 11780−11789.
19. Åhrling, K. A., and Pace, R. J. (1995) *Biophys. J. 68*, 2081−2090.
20. Sands, R. H., and Dunham, W. R. (1975) *Q. Rev. Biophys. 7*, 443.
21. Al'tshuler, S. A., and Kozyrev, B. M. (1974) *Electron paramagnetic resonance in compounds of transition elements*, 2nd rev. ed., John Wiley & Sons, New York.
22. Zheng, M., Khangulov, S. V., Dismukes, G. C., and Barynin, V. V. (1994) *Inorg. Chem. 33*, 382−387.
23. Pessiki, P. J., Khangulov, S. V., Ho, D. M., & Dismukes, G. C. (1994) *J. Am. Chem. Soc. 116*, 891−897.
24. Ono, T., Noguchi, T., Inoue, Y., Kusunoki, M., Matsushita, T., and Oyanagi, H. (1992) *Science 258*, 1335−1337.
25. Yachandra, V. K., DeRose, V. J., Latimer, M. J., Mukerji, I., Sauer, K., and Klein, M. P. (1993) *Science 260*, 675−679.
26. Messinger, J., Nugent, J. H. A., and Evans, M. C. W. (1997) *Biochemistry 36*, 11055−11060.

BI971815W